R-4

MICROSTRIP CIRCUIT ELEMENTS ON CYLINDRICAL SUBSTRATES

A. Nakatani*,** and N. G. Alexopoulos*

* University of California, Los Angeles, Los Angeles, California 90024
**Phraxos Research and Development Inc. 2716 Ocean Park Blvd., Suite 1020, Santa Monica, California 90405

ABSTRACT

Dynamic Models for a variety of miocrostrip circuits, microstrip discontinuities, and general conductor elements printed on cylindrical substrates are presented. The models accounts for radiation loss and surface wave effects. The dispersion models include the transverse current component and provide error criteria when it is omitted. Coupled lines, open ends and edge coupled resonators are also investigated.

I. INTRODUCTION

Microstrip circuits on cylindrical substrates are needed in conjunction with the design of miocrostrp antennas and microstrip antenna arrays on cylindrically shaped surfaces. In addition, a variety of waveguiding structures, surface wave launchers, and other components may be constructed with mictostrip elemints on cylindrical substrates.

This paper presents the theory and results of quasi-static as well as dynamic modelling procedures for such circuits and components. The theory accounts for arbitrary substrate parameters, inner and outer radii as well as all physical effects such as, radiation loss, substrate material loss and conductor thickness. The models are derived from the numerical solution of a Pocklington type integral equation for the circuit current distribution. The kernel of the integral equation involves the dyadic Green's function relevant to the microstrip circuit under inverstigation. In this manner a 2-D is generated for infinite, while a 3-D model is obtained for finite length microstrip structures. The precise numerical computation of the Green's function for cylindrical substrates has presented intractable difficulties in the past. Very powerful algorithms, with excellent accuracty, were developed recently for antennas printed on cylindrical sybstrates [1]-[3]. These algorithms are directly perinent and have been modified to model microstrip circuit structures on such substrates.

The derived dynamic models have been verified against quasi-static ones, equivalent limiting cases (such as two wire lines etc.) and the corresponding flat substrate microstip structures. The agreement has been found to be excellent.

The 2-D and 3-D models have been used to determine the propagation characteristics and/or the equivalent circuit parameters for the geometries shown in Figure 1. These and additional results will be discussed during the presentation.

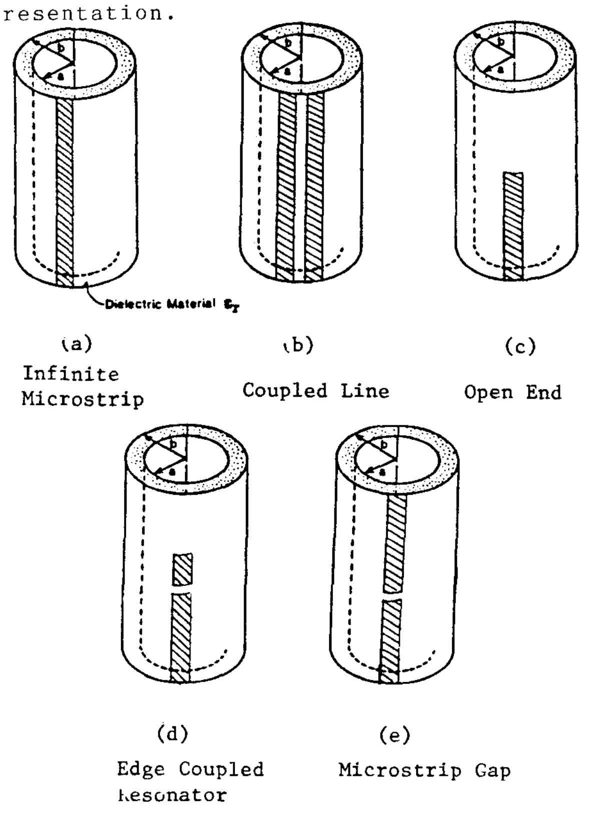

Figure 1

Microstrip Structures on a Cylindrical Substrate

II. THEORY

Galerkin's method is used to solve the unknown current density $\bar{J}$ on the microstrip elements by considering the integral equation

$$\bar{E} = \frac{1}{2\pi} \sum_{-\infty}^{\infty} \int_{-\infty}^{\infty} \bar{\bar{G}}(m,k_z) \cdot \tilde{\bar{J}}(m,k_z)\, dk_z \quad (1)$$

where $\bar{\bar{G}}(m,k_z)$ is the dyadic Green's function and the symbol "~" indicates the Fourier transform of the quantity in equation. The Galerkin's procedure descritizes equation (1) into the form

$$[V_n] = [Z_{nn'}]\,[C_{n'}] \quad (2)$$

where V_n is the equivalent voltage vector, Z is the equivalent impedance matrix, and C is the unkown constant vector element. The matrix elements $Z_{nn'}$ can be derived from

$$Z_{nn'} = \sum_{m=-\infty}^{\infty} \tilde{\bar{J}}(m,k_z) \cdot \bar{\bar{G}}(m,k_z) \cdot \tilde{\bar{J}}^{*}(m,k_z)\, dk_z \quad (3)$$

where * indicates the complex conjugate operation. When the axially oriented infinite line is considered, the axial dependency of the current distribution is considered as propagating wave. In this case, therefore, the continuous spectrum k_z is descritized for propagation constant as

$$Z_{nn'} = \sum_{m=-\infty}^{\infty} \tilde{\bar{J}}(m) \cdot \bar{\bar{G}}(m,\beta) \cdot \tilde{\bar{J}}^{*}(m) \quad (4)$$

The dispersion properties of the microstrip structure are derived by setting the determinant of impedance matrix (2) to zero for non-trivial solution and propagation constant is numerically solved.

Algorithm Description

The most crucial problem in dealing with the exact form of the Dyadic Green's function in a cylindrical configuration is the accurate evaluation of the cylindrical functions involved. The Dyadic Green's function includes the following types of terms:

$$Y_m^{(1)} = \frac{N_m(\gamma_1 a)\, J'_m(\gamma_1 b) - J_m(\gamma_1 a)\, N'_m(\gamma_1 b)}{N_m(\gamma_1 a)\, J_m(\gamma_1 b) - J_m(\gamma_1 a)\, N_m(\gamma_1 b)} \quad (5)$$

and

$$Y_m^{(2)} = \frac{N'_m(\gamma_1 a)\, J'_m(\gamma_1 b) - J'_m(\gamma_1 a)\, N'_m(\gamma_1 b)}{N'_m(\gamma_1 a)\, J_m(\gamma_1 b) - J'_m(\gamma_1 a)\, N_m(\gamma_1 b)} \quad (6)$$

where $J_m(z)$ and $N_m(z)$ are the Bessel functions of the first kind and second kind respectively. "a" and "b" correspond to the inner and outer radii of the coated cylinder. γ_1 is defined as

$$\gamma_1^2 = \varepsilon_r k_o^2 - k_z^2 \quad (7)$$

where ε_r is $\varepsilon_r = \varepsilon_r' - j\varepsilon_r''$ for lossy material.

The new numerical approach relies on a derived recurrence relation and a continued fraction representation of the Bessel functions. This method bypasses the direct computation of the Bessel functions. Instead the terms above are rewritten as follows:

$$Y_m^{(1)} = \frac{m}{\gamma_1 b} - p_m(\gamma_1 b) - \frac{p_m(\gamma_1 b) - q_m(\gamma_1 b)}{G_m^{(1)} - 1} \quad (8)$$

where

$$p_m(z) = \frac{J_{m+1}(z)}{J_m(z)} \quad \text{and} \quad q_m(z) = \frac{N_{m+1}(z)}{N_m(z)} \quad (9)$$

and

$$G_{m+1}^{(1)} = \frac{q_m(\gamma_1 a)\; p_m(\gamma_1 b)}{p_m(\gamma_1 a)\; q_m(\gamma_1 b)}\, G_m^{(1)} \quad (10)$$

with $G_o^{(1)}$ as an initial function defined as

$$G_o^{(1)} = \frac{N_o(\gamma_1 a)\; J_o(\gamma_1 b)}{J_o(\gamma_1 a)\; N_o(\gamma_1 b)}\,. \quad (11)$$

The procedure described above is highly efficient, accurate, and capable of handling any cylinder size with any thickness of coating. The developed algorithm makes possible the study of cylindrical microstrip problems that are otherwise numerically intractable since the Fourier summation of the field/current of the geometry often requires a couple of thousand terms for accurate computation of Green's function when circuit dimension is much smaller compared with the cylinder size. Therefore the direct evaluation of Bessel functions is likely to fail unless the alternative algorithm is applied to compute Green's function.

III. NUMERICAL RESULTS

The type of the problem depends on the choice of current distribution and manipulation of moment method. 2-D model requires only a circular dependency of the function while the 3-D models also requires axial dependency of the function.

By using 2-D model, low frequency behavior (quasi-static) is simulated when the wavelength is much larger than the circuit dimension and/or cylinder size. The planar geometry is approximated by using cylindrical model when the circuit dimension is much smaller than the cylinder size, independent of the size of the cylinder.

Many limitting cases have been checked to verify the accuracy of this methodology; on such case is shown in Table I. If $R=a/b<<1$, $w/(b-a)<<1$, and $\varepsilon_r \sim 1$, the situation simulates the parallel wire case for which the characteristic impedance is given by

$$Z_o = 120 \cosh(D/d) \simeq 120 \cosh(1/R) \qquad (12)$$

where D is the distance between two wires and d is the radius of each wire. As $R<<1$, the model developed herein agrees excellently with the parallel wire transmission line result.

Table 1

$R = \frac{a}{b}$	$Z_o = 120\cosh^{-1}(\frac{1}{R})$	Model
0.1	359.2	365.6
0 01	635 8	636 6
0 001	912.1	912 2
0.0001	1188 4	1188 3

The following examples shows the basic assumption of current function used for 2-D and 3-D models.

(a) 2-D modelling

The basic expansion function for the longitudinal and transverse current components are chosen as

$$J_{zi}(\phi) = \frac{\cos(k_i \phi)}{[1 - (2\phi/\delta_\phi)^2]^{1/2}} \qquad (13)$$

and

$$J_{\phi_j}(\phi) = \frac{\sin[k_\phi(\Delta - |\phi - \phi_j|)]}{\sin(k_\phi \Delta)} \qquad (14)$$

where Δ is the subsegment width of the piecewise sinusoidal basis functions, $\delta_\phi = bw$, and k_ϕ is a weighting factor. The choice of PSB function is made since the convergence rate for transverse and longitudinal Green's function is different and the use of PSB ensures the convergence for Fourier summation.

Adoption of the recurrence/continued fraction method [3] yields results for the structure shown in Figure 2 for a single microstrip line. The ratio $|I_\phi/I_z|$ is depicted in Figure 2 for $\varepsilon_r = 9.6$, $R=a/b=0.9$, and $w/H=1.0$ as a function of $k_o b$ ($k_o = 2\pi/\lambda_o$).

The circuit parameters, effective dielectric constant and characteristic impedance, are computed as

$$\varepsilon_{eff} = (\beta/k_o)^2 \qquad (15)$$

and

$$Z_o = \frac{2\pi b}{I_z^2} \sum_{-\infty}^{\infty} \tilde{J}_z V_m \tilde{J}_z^* \qquad (16)$$

where V_m is a normalized potential of the line.

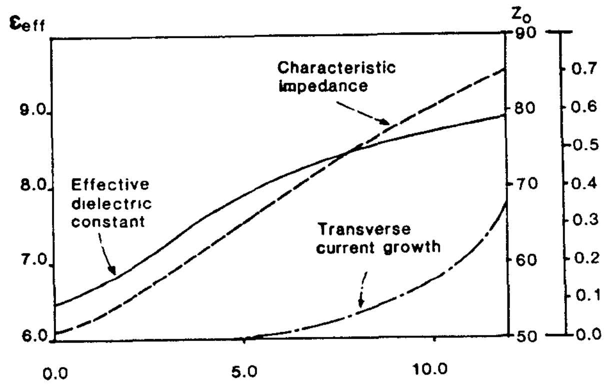

Figure 2. Frequency Dependent Microstrip Properties. ε_r=9.6, R=0.9, W/H=1.0.

(b) 3-D modelling

When the 3-D model is considered, transverse current is neglected. The longitudinal current is assumed in the form of Maxwell distribution for the transverse direction and PSB is used to expand the current density as a function of axial variable z. The current distribution on the long finete strip is used to evaluate the circuit parameters. Figure 3. shows a comparison of the 2-D and 3-D models for infinitly long microstrip line. As observed the two models agree excellently.

The presentation will also focus on the 3-D model and the numerical analysis which evolved in developing highly accurate and efficient algorithms which has been used to analyze microstrip dicsontinuities.

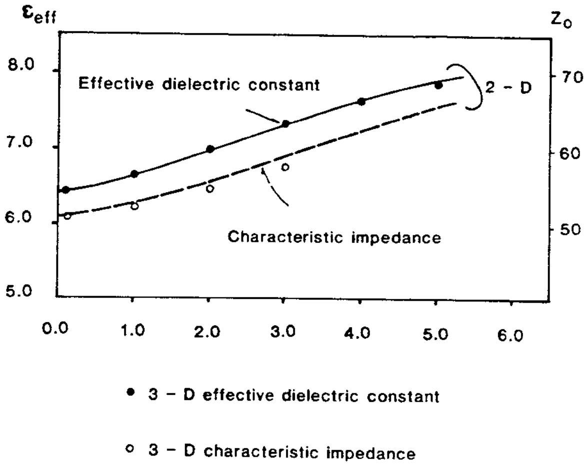

Figure 3. Comparison of 2 - D and 3 - D Simulation of Microstrip Properties. ε_r= 9.6, R=0.9, and W/H=1.0.

IV. Conclusion

The paper has presented a methodlogy which leads to the development of excellent models for the characterization of microstrip elements on cylindrical substrates. Microstrip lines and coupled lines, microstrip open end, eht edge coupled microstrip resonator, and microstrip gap have been modelled with excellent accuracy.

This research was performed under NSF Grant # ECS-86-04837 and Northrop Contract HHH 107578.

Reference

[1] N.G.Alexopoulos,P.L.E.uslengi, and N.K.Uzunoglu,"Microstrip Dipole on Cylindrical Structure," in Proc. 1981 Antenna Appl. Symp., University of Illinois, Sept. 1981.

[2] N.G.Alexopoulos, P.L.E.Uslenghi, and N.K.Uzunoglu,"Microstrip Dipole on cylindrical substrate," Electromagnetics, Special Issue on Pirnted Circuit Antennas for Microwave and Millimeter Wave Applications, vol.3, No. 3-4, pp.311-326, July-December 1983.

[3] A.Nakatani, N.G.Alexopoulos, N.K.Uzunoglu, and P.L.E.Uslenghi, "Accurate Green's Function Computation for Printed Circuit Antennas on Cylindrical Substrates," Electromagnetics, vol. 6 #3, July-September, 1986.